THE ASTROPHYSICAL JOURNAL, 524:1008–1013, 1999 October 20

PULSAR MAGNETOSPHERIC EMISSION MAPPING: IMAGES AND IMPLICATIONS OF POLAR CAP WEATHER

AVINASH A. DESHPANDE[1]
Raman Research Institute, Sadashivanagar, Bangalore 560080 India
AND
JOANNA M. RANKIN[1]
Physics Department, University of Vermont, Burlington, VT 05405
Received 1999 May 14; accepted 1999 June 5

ABSTRACT

The beautiful sequences of drifting subpulses observed in some radio pulsars have been regarded as among the most salient and potentially instructive characteristics of their emission, not least because they have appeared to represent a system of subbeams in motion within the emission zone of the star. Numerous studies of these drift sequences have been published, and a model of their generation and motion was articulated long ago by Ruderman & Sutherland; but thus far, efforts have failed to establish an illuminating connection between the drift phenomenon and the actual sites of radio emission. Through a detailed analysis of a nearly coherent sequence of drifting pulses from the pulsar B0943+10, we have in fact identified a system of subbeams circulating around the magnetic axis of the star. A mapping technique, involving a cartographic transform and its inverse, permits us to study the character of the polar cap emission map and then to confirm that it, in turn, represents the observed pulse sequence. On this basis, we have been able to trace the physical origin of the drifting subpulse emission to a stably rotating and remarkably organized configuration of emission columns, in turn traceable possibly to the magnetic polar cap gap region envisioned by some theories.

Subject headings: MHD — plasmas — pulsars: individual (B0943+10) — pulsars: general — radiation mechanisms: nonthermal

Since their discovery by Drake & Craft (1968), drifting subpulses have fascinated both observers and theorists and have often been regarded as one of the keys to understanding pulsar radio emission. Without any adequate model, early studies of prominent drifters (e.g., by Taylor & Huguenin 1971 and Backer 1973) focused on delineating the drift phenomenon. Then, the Ruderman & Sutherland (1975) model not only articulated a qualitative picture of drifting subpulses as a system of "carousel" beams circulating around the magnetic axis within the (magnetic) polar emission region, but they also attributed the rotation physically to $\boldsymbol{E} \times \boldsymbol{B}$ drift and estimated how long these circulation times would be.

While fascinating and theoretically compelling, the phenomenon has proved difficult to interpret physically. No such sequence has appeared precise enough to determine the structure and dynamics of the beams, and thus to see whether it follows any pattern that might or might not confirm the expectations of the aforementioned model. Any sight line to a star can cross the periphery of its polar emission cone at only one or two points, and it was difficult to fix accurately just where these points fell in relation to the rotational and magnetic axes. Nor was it clear to what extent the drift rates were aliased by the rotation frequency of the star. Within the Ruderman & Sutherland (1975) model, the total number of subbeams must be ascertained, or no calculation of the circulation time is possible, and thus no quantitative connection can be made with theories of the polar cap gap region. It is a telling statement on this unfortunate state of affairs that the most extensive studies of a pulsar with a highly regular drifting subpulse pattern, B0809+74, were published 25–30 years ago! (Taylor et al. 1971; Manchester, Taylor, & Huguenin 1975).

PSR B0943+10 is another pulsar in the same class, and is remarkable in other ways as well. One of a handful of pulsars discovered below 300 MHz (Vitkevich, Alexseev, & Zhuravlev 1969), it weakens markedly at higher frequencies and has never been detected above 600 MHz. Its profile evolution (and drifting subpulses) identify it as a member of the conal single (S_d) class (Rankin 1993b), and we now know that its steep spectrum is due to a sight-line traverse so peripheral that it ultimately misses the ever narrower high frequency cone. The pulsar's long sequences of drifting subpulses have prompted several different studies (Taylor & Huguenin 1971; Backer, Rankin, & Campbell 1975; Sieber & Oster 1975), all showing strong fluctuations at a frequency of 0.46 cycles per rotation period (hereafter, c P_1^{-1}), and a weaker feature near 0.07 c P_1^{-1}. Two profile modes have also been identified, a B (for "bright") mode in which subpulse drift is very prominent, and a Q (for "quiescent") mode wherein the subpulses are weaker and disorganized (Suleymanova & Izvekova 1984; Suleymanova et al. 1998). For all these reasons the pulsar's subpulse sequences are difficult to observe, and our study is based on 430 MHz observations benefiting from the high sensitivity of the large Arecibo telescope in Puerto Rico.

A short sequence of B-mode pulses is given in Figure 1, together with their average profile, and the 256 pulse fluctuation spectra in Figure 2 exhibit both the 0.46 and 0.07 c P_1^{-1} features very clearly. The former is hardly resolved, whereas the latter appears to be barely so. A harmonic connection between these two features has been debated (Taylor & Huguenin 1971; Backer et al. 1975; Sieber &

[1] Correspondence and requests for materials can be addressed to either author: desh@rri.res.in or rankin@physics.uvm.edu.

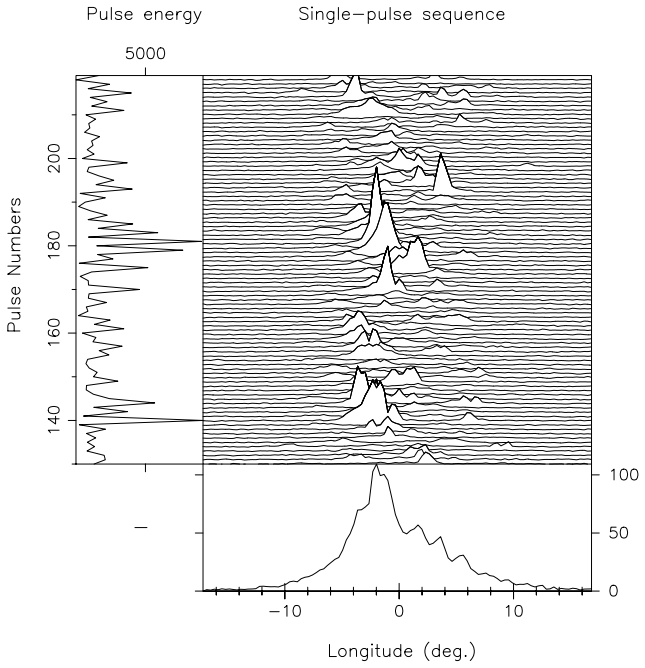

FIG. 1.—A series of individual pulses from the pulsar B0943 + 10 (*center panel*) along with their average (*bottom panel*) and energy (*left panel*) as a function of pulse number and longitude (360° longitude corresponds to 1 stellar rotation). Note the drifting subpulses, the alternate pulse modulation, and the single average profile.

Oster 1975) but never clearly determined, because of the possible ambiguities involving aliases in an ordinary longitude-resolved fluctuation spectrum, such as the one given in the figure. We have resolved the matter by exploiting the fact that the associated modulation is *continuously* sampled within the finite duration of each pulse. Therefore, we first performed a Fourier transform on the entire pulse sequence and then, from this unfolded spectrum, established that the sets of sidebands associated with the features were harmonic. This harmonic-resolved spectrum is shown in Figure 3, and will be discussed more fully in a subsequent paper (Deshpande & Rankin 1999). It can now be confidently asserted that the true phase modulation frequency is 0.5352 ± 0.0006 c P_1^{-1} (though seen at 0.46 c P_1^{-1} as a first-order alias) and that the secondary feature at 0.0710 ± 0.0006 c P_1^{-1} (a second-order alias of 1.07 c P_1^{-1}) represents its second harmonic. These frequencies vary slightly with time and are thus slightly different in our three observations, but always fall close to the 1992 October values given above.

With the aliasing resolved, it is also clear that the time interval between drift bands (usually denoted by P_3) is just $1/(0.5352 \text{ c } P_1^{-1})$ or some $1.87 P_1$ c^{-1}. Thus, just less than two rotational periods are required for subpulse emission to reappear at the same longitude, both giving the sequence its strong odd-even modulation and establishing that the actual, physical subpulse motion is from trailing to leading (or right to left) in the diagram—that is, *negative*, or in the direction of decreasing rotational longitude.

The fluctuation spectra of Figures 2 and 3 also show a pair of symmetrical sidebands associated with the primary feature. These sidebands fall 0.027 c P_1^{-1} higher and lower

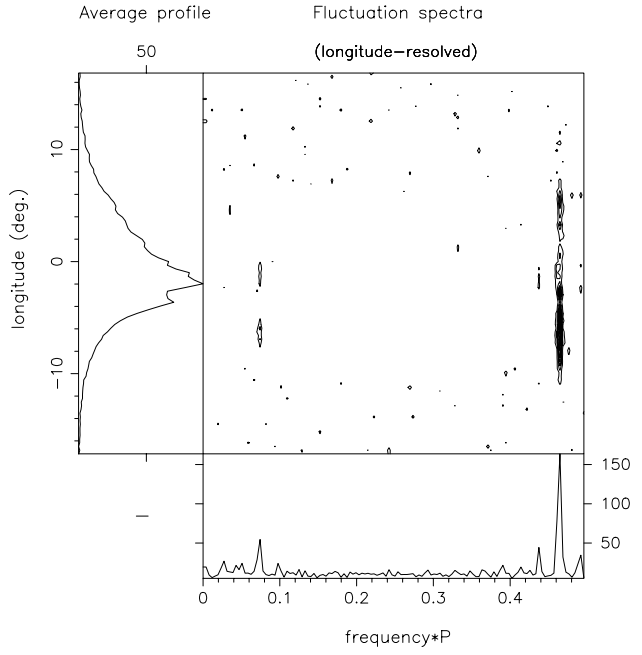

FIG. 2.—Fluctuation–spectral power (*center panel*) as a function of longitude and frequency as well as the integral spectrum (*bottom panel*). Note the primary and secondary features at about 0.46 and 0.07 c P_1^{-1} as well as the symmetrical sidebands around the former.

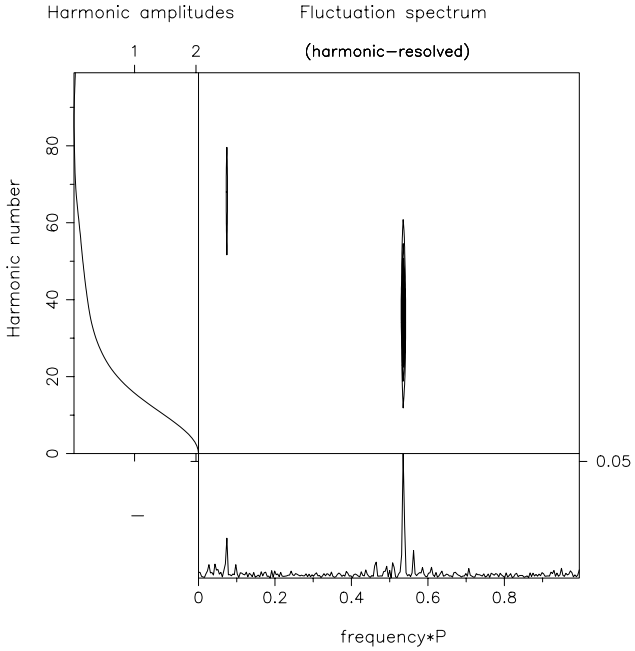

FIG. 3.—Fluctuation spectrum of a continuously sampled time sequence reconstructed from the (gated) single-pulse sequence used in Fig. 2. The spectrum is presented in a matrix form with each row showing a section of the spectrum between n/P_1 and $(n+1)/P_1$ for harmonics $n = 0, 1, 2, \ldots$ of the rotation frequency $1/P_1$. The harmonics at n/P_1 are shown separately (*left panel*) and are essentially the Fourier components of the average profile. All other frequency components (up to $100/P_1$) are given as a contour plot (*center panel*), and the column sum of these components, collapsed into a $1/P_1$ interval (*bottom panel*), can be compared directly with Fig. 2. Note that the principal feature now falls at an (unaliased) frequency of about 0.535 c P_1^{-1}. Note also that whereas the Fourier amplitudes of the principal feature peak at about harmonic (row) number 35 (corresponding to a P_2 value of some 10°.5), those of the secondary feature peak around number 70, thus demonstrating their harmonicity.

than the principal fluctuation and represent an amplitude modulation *on* the phase modulation. This circumstance, viewed along with the remarkable stability of the phase fluctuation, demands that these features also have a harmonic relationship with the fundamental fluctuation frequency, so we are not surprised to find that $(0.535 \text{ c } P_1^{-1})/(0.027 \text{ c } P_1^{-1}) = 20.01 \pm 0.08$, which is an integer, 20, to well within the errors. The entire modulation cycle is then just 20 times $1.87P_1$, or some 37.35 ± 0.02 periods, and this circumstance is beautifully confirmed in Figure 4, where the full sequence has been folded at this period.

We have also studied the geometry and polarization of the pulsar in unprecedented detail. All the available mean profiles (seven frequencies between 25 and 430 MHz) were used to model the star's conal beam geometry, thus fixing the angles that the magnetic axis and sight line, respectively, make with the rotation axis. Four different configurations were explored, corresponding to both inner and outer cones (Rankin 1993a, 1993b; Mitra & Deshpande 1999) and to poleward and equatorward sight-line traverses, respectively. All show that at 430 MHz the sight line makes an exceedingly tangential traverse through the emission cone—at close approach still some 102% of the half-power radius of the cone. Only a poleward traverse could be reconciled with both the observed polarization angle sweep rate of some $-3° \text{ deg}^{-1}$ (Suleymanova et al. 1998) and the requisite magnetic azimuth interval (18°) between adjacent subpulses,[2] which then also fixes the actual, physical sense of rotation of the nearer (rotation) axis as clockwise. We calculate the magnetic azimuth interval between adjacent subpulses on the basis of (*a*) their longitude separation and (*b*) the polarization angle rotation between them (Radhakrishnan & Cooke 1969), obtaining values of 18° independent of (inner or outer) conal radius. Clearly, entities at 18° intervals are 20 in number, implying a vigesimal beam system circulating in magnetic azimuth.

Pulsar researchers have long tended to view drifting subpulses as a pattern of "carousel" beams (Ruderman & Sutherland 1975; Sieber & Oster 1976) rotating around the magnetic axis, but heretofore it had not been possible to verify this picture either by tracing a given beam through its circuit or by establishing the total number of beams. We see that our observations and analysis of PSR 0943+10 now give clear signatures of 20 beams, rotating counterclockwise around its emitting magnetic axis in a total time $\hat{P}_3$ of some 37 periods or 41 s. Furthermore, we understand the pulsar's emission geometry sufficiently well that we can transform the received sequence from the observer's frame into a frame that is rotating about the magnetic axis of the pulsar. This cartographic transform then maps the intensity as a function of longitude (with respect to that of the magnetic axis) $\phi - \phi_0$ and pulse number $k - k_0$ into magnetic-polar colatitude R and azimuth θ (rotating with period $\hat{P}_3$). Successive pulses then sample the intensity along successive chordlike traverses (corresponding to different azimuth intervals) through the rotating beam pattern.

Applying this cartographic transformation to the B-mode portion of our 1992 observations, Figure 5 shows the average configuration of the 20 subbeams that produce the drift sequence. The rotation of adjacent beams through our sight line produces the secondary phase modulation, and the periodic pattern of varying beam intensities gives it its tertiary amplitude modulation. We find that the subbeams vary, both in intensity and in azimuthal spacing, over 100 s timescales. Closely spaced beams tend to be weaker, and some beams are observed to bifurcate temporarily, but the 20-fold pattern is always maintained strongly as a stable configuration. The elongated shape of the beams can be understood as a result of truncation, as most of the emission falls inside the 430 MHz sight-line traverse. Indeed, a similar map at a much lower frequency (111.5 MHz), where we expect the sight line to sample emission interior to the one above, shows a more nearly circular subbeam shape.

How sensitive are the conclusions drawn from the cartographic transform to any assumptions in the analysis? The mapping procedure is exquisitely sensitive to the circulation time, and only a little less so to the longitude of the magnetic axis, to the polarization angle sweep rate, and to the angles specifying the colatitude of the magnetic axis and sight-line impact angle. Overall, these parameters scale the map—or utterly distort it. However, the forward transform used to construct the maps has a true inverse transform, and this inverse cartographic transform can be used to play back a map in order to produce an artificial pulse sequence. Only when this artificial sequence correlates in full with the observed sequence do we take the map as correct. Indeed, we have carried out such inverse transforms iteratively in a kind of search mode to refine each of the requisite parameters, and a completely consistent picture is found in observations from 1974 and 1992 at 430 MHz and from 1990 at 111 MHz.[3]

The overall structure of the radio beam of 0943+10 provides new insight into the physical nature of pulsar emission. Its 20 subbeams rotate almost rigidly, maintaining their number and spacing despite perturbations tending both to bifurcate a given beam and to merge adjacent ones, and we find an almost identical subbeam configuration at the two frequencies. These circumstances suggest that the subbeam emission region lies along bundles of magnetic field lines (or plasma columns) having "feet" within a certain annulus on the polar cap, wherein charges are accelerated at some distance above the stellar surface, and radiation occurs at progressively higher altitudes for lower and lower frequencies. We can thus peer at the activity at the feet of the plasma columns and possibly monitor changes viewable at intervals of the circulation time.

The subbeam radiation we observe, estimated to be emitted at some 100–300 km height, then reflects processes occurring at lower altitudes along these ultramagnetized plasma columns—indeed, some fully down at the surface where the electric fields caused by the star's rotation appear. The foot of each subbeam column moves around the magnetic axis, so we cannot appeal to any surface features or fixed hot spots as their cause. The entire rotating subbeam pattern, averaged over time, represents a hollow cone beam of emission, which is emitted along the magnetic field direction at a particular height for a given frequency. Signatures of such conical beams are encountered in most pulsars, and

[2] The inner cone solution corresponds to α and β some 11°.6 and $-4°.3$, respectively, and all of our calculations are based on these values. Other solutions such that $\sin \alpha / \sin \beta \approx -3° \text{ deg}^{-1}$ only change the overall scale of the map.

[3] Moving images of these sequences can be viewed at web sites with the following URL addresses: http://www.rri.res.in/~desh and http://www.uvm.edu/~jmrankin.

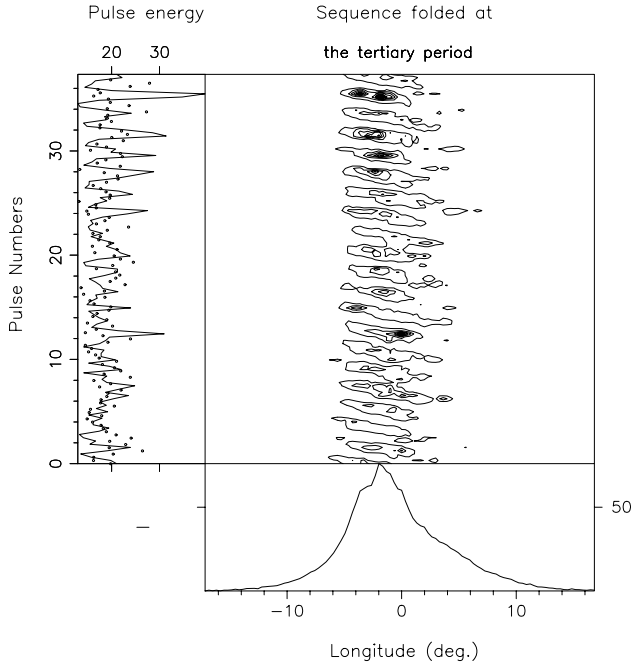

FIG. 4.—Pulse sequence folded at the full 37.35 period modulation cycle (*center panel*). Twent emission centers can be readily identified, and their relative intensity is shown as a function of longitude (*bottom panel*) and modulation phase in units of pulse number (*left panel*). For comparison, the dots in the latter show the result using a tertiary period that is 2% different from the correct one.

accurately reflect the angular dimension of the magnetic polar cap (Rankin 1993a).

Nonetheless, we have little guidance about where the feet of these plasma columns will fall on the polar cap. Clearly, the radius of the active polar cap $r_{\rm PC}$ scales as the square root of the star's radius to that of the light cylinder, $r_{\rm PC} = \epsilon r_*(2\pi r_*/cP_1)^{1/2} \sim 145\epsilon P_1^{-1/2}$ m (assuming $r_* \approx 10$ km), and values of ϵ near unity have been taken to describe the outside edge of the emission pattern.[4] Therefore, polar cap features corresponding to the subbeam columns would have separations of some 45ϵ m and individual sizes of some 20ϵ m across. These dimensions would increase only a little even if the feet of the plasma columns happened to be a few stellar radii away from the star's surface. Interpreted another way, our estimate of the angular width of the subbeams (based on the magnetic colatitude spread seen in the map at 111.5 MHz) suggests Lorentz factors $\gamma > 200$. We note again that our extremely tangential sight line permits us to sample only the outermost portion of each subbeam at 430 MHz, and so only this outer portion can be mapped down onto the polar cap.

Ruderman & Sutherland (1975, hereafter R&S) nearly 25 years ago identified the drift-associated subbeams with electrical breakdowns (or "sparks") in the polar cap gap region, and argued that their circulation was due to $\boldsymbol{E} \times \boldsymbol{B}$ drift. Although the major standpoint of their model, that even the enormous electric fields that must be generated would be inadequate to overcome the binding energy of the positive charges (such as iron ions) at the neutron star surface, now seems untenable (Jones 1985, 1986), closely related models are still in active discussion (e.g., Usov & Melrose 1995; Zhang & Qiao 1996; Zhang 1997). It is noteworthy that no completely independent model of subpulse drift seems to exist, and our maps do suggest a qualitative picture something like the model R&S envisioned. Any subpulse drift model needs to explain first why subpulse scale structures occur, and then why they circulate in azimuth. According to Ferraro's theorem (Ferraro & Plumpton 1966), the open field region above the polar cap must rotate with, but perhaps more slowly than, the star (so that, for an inertial observer, they would both rotate in the same direction); thus, in the pulsar's frame the regions will rotate oppositely, as is observed for 0943 + 10.[5]

Two quantitative features of the R&S model are noteworthy. First, their gap height is some 50 m, which is also related, in the model, to the scale over which an active "spark" or plasma column inhibits the formation of others, and the 45ϵ m we infer is fully consistent with this value. Second, the observed circulation time can also be reconciled with their model. $\hat{P}_3$, at polar cap radius r_s, for drifting at velocity $\boldsymbol{E} \times \boldsymbol{B}/B^2$, can be written as $\hat{P}_3 = 2\pi r_s B/\langle E\rangle P_1$, where B and $\langle E\rangle$ are the magnetic field and the average radial electric field in the gap region. $\langle E\rangle$, in turn, depends on the gap potential drop ΔV and the spark distance from the edge of the cap, so that the average field is perhaps some $\langle E\rangle = \Delta V/2(r_{\rm PC} - r_s)$ (cf. R&S, eq. [30]). Assuming that the pulsar's magnetic field is correctly computed as a surface value (see de Jager & Nel 1988, eq. [1]), then B is 2×10^{12} G, P_1 is 1.1 s, and thus $\hat{P}_3$ can be as large as $37P_1$ only if $(r_{\rm PC} - r_s) \sim r_s$ and $\Delta V/\epsilon^2$ is well less than 10^{12} V. In any case, the $\langle E\rangle$ in the acceleration region is required to be $\sim 3 \times 10^9\epsilon$ V m^{-1}, for the circulation to be due to $\boldsymbol{E} \times \boldsymbol{B}$ drift.

Our maps suggest that the angular velocity associated with the circulation is nearly constant across the radial extent of the subbeams, because no azimuthal shear is observed within the subbeams. The exact origin and significance of any possible dependences of $\hat{P}_3$ on radius and other parameters needs to be understood, and similar estimates of circulation time in other pulsars (with different rotational parameters and geometries) should help to define this issue. The finely tuned stability of the pattern observed in this pulsar has more to tell. It is unlikely that the remarkably periodic and stable arrangement would be possible if the required spacing of subbeams were not an integral submultiple of the circumference of the ring on which they appear to arrange themselves. The particular characteristics of the pulsar B0943 + 10 may therefore result from a critical combination of parameters: namely, its rotation period, emission geometry, magnetic field strength, and subbeam spacing, which in turn could be determined by the gap height. It should not, therefore, be surprising to find that this remarkable configuration is indeed an unusual one.

Nevertheless, averaged over many circulation times, the emission pattern of 0943 + 10 conclusively demonstrates the existence of the hollow conical emission beams long attributed to many pulsars through less direct means. The subbeam columns must be nearly axially symmetric with respect to the magnetic axis, because any significant devi-

[4] For example, ϵ is $(2/3)^{3/4}$ in Ruderman & Sutherland (1975) and 1.5 in Rankin (1990), respectively.

[5] That the polar cap drift lags the star's rotational speed may, then, be evidence for a gap somewhere between the emission region and the stellar surface, but it gives no indication about whether positive (or negative) charges would be accelerated outward, or, in R&S's terms, whether the star is a pulsar or an antipulsar (Ruderman 1976).

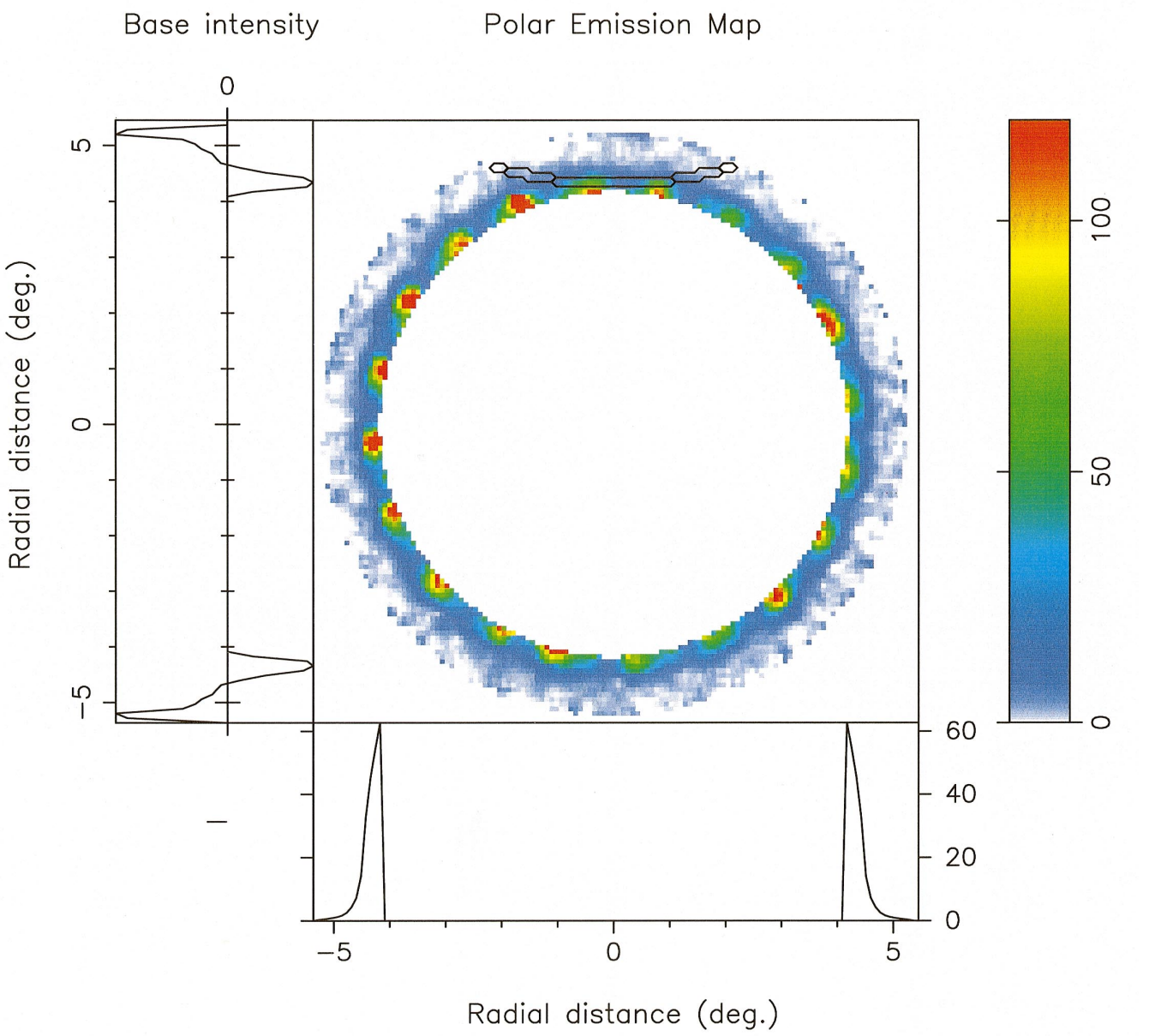

FIG. 5.—Results of the cartographic transformation. The individual-pulse sequence has been mapped onto a rotating frame centered on the magnetic axis. Azimuthal average and minimum (unfluctuating base) intensity as a function of magnetic colatitude are given in the bottom and left panels, respectively. Note the 20 emission centers and their somewhat elongated shape. A portion of the sight-line traverse is also indicated at the top of the figure.

ation would require a contrived situation to reproduce the periodicities and polarization that we observe. Models in which only a part of the polar cap is active (e.g., Arons & Scharlemann 1979; Arons 1979) are incompatible with these results.

The central conclusion to be drawn from our subbeam mapping of the pulsar B0943+10 is that the emitting pattern, which is so very stable over hundreds of seconds or many circulation cycles, is frozen neither to the fields nor to the stellar surface. We must then ask where, physically, the "memory" of the subbeam pattern is carried in this system of charges and particle currents despite the circulation. The detailed structure that we have mapped traces the activity at the feet of the emission columns and represents the first direct measurements of some of its parameters—such as the locations, size, and movement of the underlying pattern—reflecting the electrodynamics not very far from the stellar surface. The overall continuity of the emission, implicit in the stability of the pattern over many circulation periods, demands a remarkable collective steadiness at every stage of the emission process—such as generation and acceleration of particles and *coherent* amplification.

In summary, the pulsar 0943+10 exhibits an exquisitely stable drifting subpulse pattern in its B-mode sequences with a nearly even-odd fluctuation frequency of about 0.53 c P_1^{-1}. Upon first establishing the aliasing order of this feature, and then accurately modeling the star's emission geometry, we found that the two sideband features resulted from a tertiary amplitude modulation on the secondary phase modulation. The remarkable precision of the modulation rates argues for a system of subbeams circulating around the magnetic axis, prompting the use of a novel cartographic transform to map the subbeam structure responsible for the pulse-to-pulse fluctuations. The detailed

parameters of the circulating subbeams allow quantitative assessment of the possible interpretation in terms of the system of rotating sparks on the polar cap as suggested in the Ruderman & Sutherland (1975) model. The current analysis holds considerable promise for studying the emission properties in other pulsars and for assessing physical emission theories.

We thank Vera Izvekova, Svetlana Suleymanova, and N. Rathnasree for help with the observations, and V. Radhakrishnan and Rajaram Nityananda for their insightful, helpful comments and many useful suggestions for improving the manuscript. We are also grateful to Malvin Ruderman, Alice Harding, and Jonathan Arons for useful discussions. Portions of this work were carried out under US National Science Foundation grants AST 89-17722 and INT 93-21974. Arecibo Observatory is operated by Cornell University under contract to the US National Science Foundation.

REFERENCES

Arons, J. 1979, Space Sci. Rev., 24, 437
Arons, J., & Scharlemann, E. T. 1979, ApJ, 231, 854
Backer, D. C. 1973, ApJ, 182, 245
Backer, D. C., Rankin, J. M., & Campbell, D. B. 1975, ApJ, 197, 481
de Jager, O. C., & Nel, H. I. 1988, A&A, 190, 87
Deshpande, A. A., & Rankin, J. M. 1999, in preparation
Drake, F. D., & Craft, H. D., Jr. 1968, Nature, 220, 231
Ferraro, V. C. A., & Plumpton, C. 1966, Magneto-Fluid Mechanics (London: Oxford Univ. Press), 23
Jones, P. B. 1985, Phys. Rev. Lett., 55, 1338
———. 1986, MNRAS, 218, 477
Manchester, R. N., Taylor, J. H., & Huguenin, G. R. 1975, ApJ, 196, 83
Mitra, D., & Deshpande, A. A. 1999, A&A, 343, 906
Radhakrishnan, V., & Cooke, D. J. 1969, Astrophys. Lett., 3, 225
Rankin, J. M. 1990, ApJ, 352, 247
———. 1993a, ApJ, 405, 285
———. 1993b, ApJS, 85, 145
Ruderman, M. A. 1976, ApJ, 203, 206
Ruderman, M. A., & Sutherland, P. G. 1975, ApJ, 196, 51
Sieber, W., & Oster, L. 1975, A&A, 38, 325
———. 1976, ApJ, 210, 220
Suleymanova, S. A., & Izvekova, V. A. 1984, Soviet Astron., 28, 32
Suleymanova, S. A., Izvekova, V. A., Rankin, J. M., & Rathnasree, N. 1998, J. Astrophys. Astron., 19, 1
Taylor, J. H., & Huguenin, G. R. 1971, ApJ, 167, 273
Taylor, J. H., Huguenin, G. R., Hirsch, R. M., & Manchester, R. N. 1971, Astrophys. Lett., 9, 205
Usov, V. V., & Melrose, D. B. 1995, Australian J. Phys., 48, 571
Vitkevich, V. V., Alexseev, Yu. I., & Zhuravlev, Yu. P. 1969, Nature, 224, 49
Zhang, B. 1997, ApJ, 478, 313
Zhang, B., & Qiao, G. J. 1996, A&A, 310, 135